NMR investigation of spin fluctuations in the itinerant-electron magnetic compound $Sr_{1-x}Ca_xCo_2P_2$

Masaki Imai,[1,2] Chishiro Michioka,[1] Hiroaki Ueda,[1] and Kazuyoshi Yoshimura[1,3,*]

[1]*Department of Chemistry, Graduate School of Science, Kyoto University, Kyoto 606-8502, Japan*

[2]*Advanced Science Research Center, Japan Atomic Energy Agency, Tokai 319-1195, Japan*

[3]*Research Center for Low Temperature and Materials Sciences, Kyoto University, Kyoto 606-8501, Japan*

(Received 20 July 2016; revised manuscript received 27 January 2017; published 15 February 2017)

We took ^{31}P NMR measurements of mainly paramagnetic phase $Sr_{1-x}Ca_xCo_2P_2$ ($0 \leqslant x \leqslant 0.5$) to reveal the itinerant-electron metamagnetic transition, and of its magnetically ordered phase ($0.7 \leqslant x \leqslant 1$), and characterized their spin fluctuations by estimating the spin fluctuation parameter T_0 corresponding to the width of the spin fluctuation in the spectrum in frequency space. $SrCo_2P_2$ has a quasi-two-dimensional uncollapsed tetragonal (ucT) cell without interlayer P-P bonds, whereas $CaCo_2P_2$ has a three-dimensional collapsed tetragonal (cT) cell with P-P bonds. The *ab*-in-plane component of T_0 is much larger than the out-of-plane component in $SrCo_2P_2$. As x increases from 0 to 0.5, the in-plane component of T_0 decreases proportionally with the metamagnetic transition field. In the antiferromagnetic cT phase ($0.7 \leqslant x \leqslant 1$), T_0 is constant and spin fluctuations show an isotropic character in contrast to their behavior in the paramagnetic ucT phase ($0 \leqslant x \leqslant 0.5$). These results indicate that the in-plane spin fluctuations due to the quasi-two-dimensional crystal structure play a significant role in the metamagnetic transition of this system.

DOI: 10.1103/PhysRevB.95.054417

I. INTRODUCTION

The quantum phase transition, currently a main topic in the field of condensed matter physics, has been extensively investigated, especially since the discovery of unconventional superconductivities in, for example, high-T_c cuprates and ferromagnetic uranium compounds, and high-T_c iron pnictides. Among the iron pnictides, the $ThCr_2Si_2$-type layered compounds have been extensively studied [1–3]. The parent compound $BaFe_2As_2$ shows a stripe-type antiferromagnetic order, with superconductivity appearing by suppressing the magnetic ordering through applying physical pressure or substitutions K and P for Ba and As, respectively. In this system, antiferromagnetic spin fluctuations play a crucial role for superconductivity to occur [4–6].

In cobalt pnictides with a $ThCr_2Si_2$ structure, they exhibit itinerant-electron magnetism without superconductivity. For example, from magnetization and NMR measurements and analysis, $BaCo_2As_2$ and $SrCo_2As_2$ were reported as being enhanced Pauli paramagnets with ferromagnetic interaction [7–10]. In addition, the temperature dependence of the magnetic susceptibility of $SrCo_2As_2$ has a characteristic maximum at 115 K without magnetic ordering [9,10]. These cobalt pnictides have a ferromagnetic interaction in contrast to the stripe-type antiferromagnetic $BaFe_2As_2$. Depending on the A cation, ACo_2P_2 (A = La, Ca, Sr, and Ba) shows a variety of itinerant-electron magnetism with a dominantly ferromagnetic interaction in a Co-P tetrahedral layer. $SrCo_2P_2$ is an exchange-enhanced Pauli paramagnet and its magnetic susceptibility exhibits a Curie-Weiss-like temperature dependence at high temperatures and broad maximum behavior at 110 K [11,12]. Furthermore, an itinerant-electron metamagnetic transition from the Pauli paramagnetic to the ferromagnetic state appears when a high magnetic field of 60 T is applied [13]. $LaCo_2P_2$ and $CaCo_2P_2$ have a stronger ferromagnetic interaction and hence have a ferromagnetic ordering in the Co-P layer. The former exhibits ferromagnetic ordering [14], and the latter A-type antiferromagnetic ordering because of an antiferromagnetical interaction between neighboring Co-P layers [15].

From the view point of interlayer molecular bonding, these $ThCr_2Si_2$-type compounds are classified into two types: one is an uncollapsed tetragonal (ucT) structure without X-X bonds (X = anion), the other is a collapsed tetragonal (cT) structure with X-X bonds [16]. In $Sr_{1-x}Ca_xCo_2P_2$ and $SrCo_2(P_{1-x}Ge_x)_2$, the structural change from ucT for $x = 0$ to cT for $x = 1$ occurs at a certain x, and the magnetic properties change considerably as the X-X bonds develop [11,17]. The ground state of the ucT phase in $Sr_{1-x}Ca_xCo_2P_2$ ($0 \leqslant x \leqslant 0.5$) is the exchange-enhanced Pauli paramagnetic metal. The itinerant-electron metamagnetic transition is also observed in these phases similar to the mother compound $SrCo_2P_2$ [13]. In cT phases with $0.5 < x \leqslant 1$, the interlayer antiferromagnetic coupling develops and the ground state becomes antiferromagnetic with ferromagnetic ordering in the Co-P layer. In addition, from the temperature dependence of the magnetic susceptibility and heat capacity, a ferromagnetic quantum critical point was discovered at $x = 0.675$ in $SrCo_2(P_{1-x}Ge_x)_2$ [17,18].

$SrCo_2P_2$ and its substituted system are attractive as metallic quantum ferromagnetic systems because both feature a first-order-metamagnetic transition and a quantum critical point where a second-order phase transition has been suppressed at 0 K. The metamagnetic transition of $SrCo_2P_2$ is sensitive to carrier doping and disappears with only 5% of La for Sr or 10% of Ge for P substitution [19]. Moreover, the metamagnetic transition remains up to $x = 0.5$ in the isovalently substituted $Sr_{1-x}Ca_xCo_2P_2$ system, in which the transition field decreases as x increases to 0.5 [13].

We measured the microscopic magnetic properties of $Sr_{1-x}Ca_xCo_2P_2$ in NMR experiments to reveal the mechanism underlying the metamagnetic transition. Near a ferromagnetic quantum critical point, treatment and understanding of the

*kyhv@kuchem.kyoto-u.ac.jp

electron correlation are essential in explaining the characteristic quantum critical behavior. The electron correlation has been treated using the theory of spin fluctuations [20], which succeeds in explaining the behavior of weakly (anti)ferromagnetic metals. Starting with the self-consistent renormalization (SCR) theory of spin fluctuations, the quantum critical behavior in physical properties was clarified by Moriya [20], and that work was extended later by Millis [18]. In the SCR theory, the dynamical susceptibility is described as a double-Lorentzian spectrum in the wave vector ($\boldsymbol{q}$) space and the frequency (ω) space using spin-fluctuation parameters T_A and T_0 [20]. The estimation of these spin-fluctuation parameters is useful in characterizing itinerant-electron ferromagnets [21]. Spin fluctuations can be directly observed through inelastic neutron diffraction and NMR measurements. NMR probes low-frequency spin dynamics over NMR timescales. The spin-lattice relaxation rate in NMR is related to the wave vector $\boldsymbol{q}$ summation of the imaginary part of the dynamical susceptibility.

In a previous paper [22], we determined the parameters of the ferromagnetic metal $LaCo_2P_2$ from NMR results by applying the SCR theory and by the magnetization measurement using Takahashi's theory [21], developed from SCR framework. We concluded that $LaCo_2P_2$ has three-dimensional spin fluctuations and can be understood in the combined framework of the above theories.

In this paper, we present microscopic magnetic properties of single crystals of ACo_2P_2 (A= Ca and Sr) and polycrystalline samples of $Sr_{1-x}Ca_xCo_2P_2$. We measured the Knight shift and nuclear spin-lattice relaxation rate related to the static magnetic susceptibility and the spin fluctuation of the vertical component to the field direction, respectively. In addition, we analyzed the NMR data using the SCR theory and obtained the spin-fluctuation parameter T_0, which characterizes the spectral width of the dynamical spin susceptibility in frequency space. We found that $SrCo_2P_2$ has anisotropic spin fluctuations, and T_0 estimated in the Co-P plane scales with the metamagnetic transition field.

II. EXPERIMENTAL METHOD

Single crystals of $SrCo_2P_2$ and $CaCo_2P_2$ were prepared by the tin flux method. The solid solution samples of $Sr_{1-x}Ca_xCo_2P_2$ were synthesized by a conventional solid-state reaction [13]. The polycrystalline samples were ground to a fine powder using mortar and pestle, and then the powder was aligned magnetically using a 5-T field at room temperature and fixed in Stycast 1266 epoxy. The magnetic easy axis of paramagnetic $Sr_{1-x}Ca_xCo_2P_2$ ($x \leqslant 0.5$) is in the tetragonal ab plane; the c aligned samples were obtained with the powder sample rotated about a perpendicular axis to the magnetic field. For the antiferromagnetic $Sr_{1-x}Ca_xCo_2P_2$ ($x > 0.5$), their magnetic easy axis is along the c axis; c-aligned samples were obtained with the powder sample placed in the magnetic field. The c-axis crystal orientation in the fixed samples was confirmed from x-ray powder diffractometry taken in the Bragg-Brentano geometry.

The temperature-dependent magnetizations $M(T)$ of $Sr_{1-x}Ca_xCo_2P_2$ were measured using a magnetometer (MPMS-XL, Quantum Design) at the Research Center for Low Temperature and Materials Sciences, Kyoto University. With the magnetic field H applied successively along the a and c axes, the magnetizations M of the samples were measured at 1 T. Field-swept ^{31}P NMR spectra were measured by the spin-echo method using a standard phase-coherent-type spectrometer. The ^{31}P nucleus has a nuclear spin $I = 1/2$ and a gyromagnetic ratio $^{31}\gamma = 17.237$ MHz/T. The Knight shift ^{31}K is defined as $^{31}\mathrm{K} = (H_{\mathrm{ref}} - H_{\mathrm{obs}})/H_{\mathrm{obs}}$, where $H_{\mathrm{ref}} = \nu_{\mathrm{ref}}/^{31}\gamma$; the operating frequencies ν_{ref} were 60.20 MHz for single crystals of $SrCo_2P_2$ and $CaCo_2P_2$ and 32.10 MHz for the c-aligned powder samples. The nuclear spin-lattice relaxation time T_1 was measured by the inversion-recovery method using the echo signal following a spin-inverting π pulse. For all samples, nuclear magnetization recovery followed a simple single exponential function over the entire temperature range.

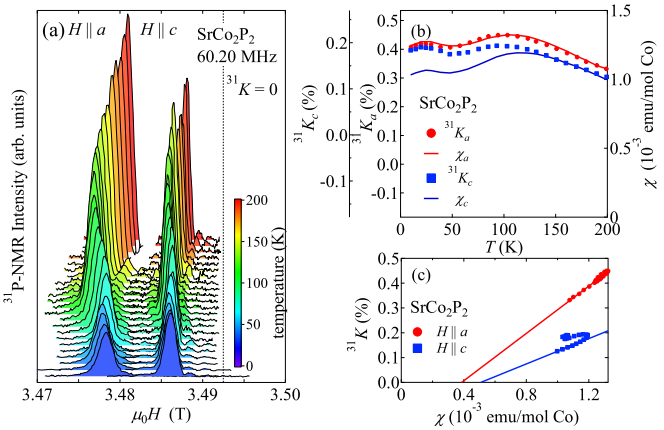

FIG. 1. NMR results for static susceptibility in single crystals of $SrCo_2P_2$. (a) Normalized field-swept ^{31}P-NMR spectra with the applied field $H \parallel a$ and $H \parallel c$ at 60.20 MHz. (b) Temperature dependence of the Knight shift and magnetic susceptibility. The red circles and blue squares distinguish $^{31}K_a$ and $^{31}K_c$, respectively. The red and blue lines mark χ_a and χ_c. (c) K versus χ plots for each field direction. The red and blue lines represent linear fits over ranges 4.2–200 K and 130–200 K, respectively.

III. RESULTS AND DISCUSSION

A. Single crystals of $SrCo_2P_2$

Field-swept ^{31}P NMR measurements for single crystals were performed with operating frequency $\omega = 60.20$ MHz for an applied magnetic field parallel to a and to c. The normalized spectra at each temperature [Fig. 1(a)] show a very sharp single peak for both field directions $H \parallel a$ and $H \parallel c$. The Knight shifts for $H \parallel a$ ($^{31}K_a$) and $H \parallel c$ ($^{31}K_c$) are obtained from the peak position of the spectrum. The temperature dependence of $^{31}K_a$, $^{31}K_c$, and the magnetic susceptibility χ [Fig. 1(b)] show that both $^{31}K_a$ and $^{31}K_c$ have two maxima at 25 and 100 K as for the magnetic susceptibility. The value of $^{31}K_a$ is double that for $^{31}K_c$, although the anisotropy of magnetic susceptibility is not so large because the hyperfine coupling constant becomes anisotropic. Figure 1(c) shows $^{31}K_i$ versus χ_i ($i = a,c$) plots for various values of T. Both $\chi(T)$ and $K(T)$ decompose into a T-dependent d-spin component and other T-independent components. Because

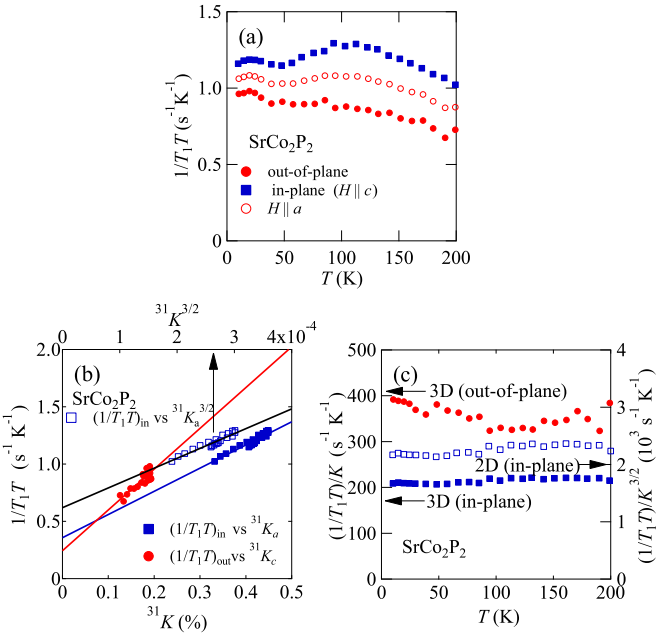

FIG. 2. Dynamical magnetic properties in single crystals of $SrCo_2P_2$. (a) Temperature dependence of $1/T_1T$. The open red circles, the solid blue squares, and the solid red circles represent $(1/T_1T)_a$, $(1/T_1T)_{in} = (1/T_1T)_c$, and $(1/T_1T)_{out} = 2(1/T_1T)_a - (1/T_1T)_c$, respectively. (b) $1/T_1T$ versus K plots. The solid red circles and solid blue squares distinguish $(1/T_1T)_{in}$ versus K_a, $(1/T_1T)_{out}$ versus K_c (bottom scale), and the open blue squares mark $(1/T_1T)_{in}$ versus $K_a^{3/2}$ (top scale), respectively. The red, blue, and black lines represent linear fits to the data. (c) Temperature dependence of $1/T_1TK$ (left scale) and $1/T_1TK^{3/2}$ (right scale).

the T-independent components of K are relatively smaller than the d-spin component $K_d(T)$, $K(T)$ is roughly regarded as $K_d(T)$. For $H \parallel a$, the K-χ plot shows strong linearity over the entire temperature range, and the hyperfine coupling constant A_a is estimated as 26.6 ± 0.9 kOe/μ_B. For $H \parallel c$, the slope of the K-χ plot changes at approximately 110 K, with the slope being independent of T below 100 K and again above 130 K.This is probably because magnetic impurities easily affect χ, especially at low temperature.For the liner fit of the K–χ plot over ranges 130–200 K, the hyperfine coupling constant A_c is estimated as 16.8 kOe/μ_B, which is considerably larger than for A_a. In $LaCo_2P_2$, A_a was found to be larger than A_c [22].

Figure 2(a) shows the temperature dependence of the nuclear-spin-lattice relaxation rate divided by temperature $1/T_1T$. The temperature dependence of $1/T_1T$ for both field directions $H \parallel a$ and $H \parallel c$ also shows two maxima at 25 and 100 K, as observed with K and χ. The $1/T_1T$ reflects the wave vector $\boldsymbol{q}$ summation of the field-vertical component of the imaginary part of the dynamical electron spin susceptibility $\chi(\boldsymbol{q},\omega)$. For Pauli paramagnetic metals, $1/T_1T$ obeys the Korringa relation ($1/T_1T \propto K^2$). When the magnetic interaction is ferromagnetically enhanced, $1/T_1T$ is predicted to be proportional to K in the three-dimensional ferromagnet or $K^{3/2}$ in the two-dimensional ferromagnet according to the SCR theory of spin fluctuations [20]. The in-plane and out-of-plane components of the spin fluctuations are defined as

$$(1/T_1T)_{in} = (1/T_1T)_c, \tag{1}$$

$$(1/T_1T)_{out} = 2(1/T_1T)_a - (1/T_1T)_c, \tag{2}$$

respectively. Figure 2(b) shows the three- and two-dimensional analyses in accordance with the SCR theory as plots of $(1/T_1T)_{in}$ versus K_a and $K_a^{3/2}$, and $(1/T_1T)_{out}$ versus K_c. The d-spin component of $(1/T_1T)$ is estimated from the y-axis intercept obtained from linear fits [Fig. 2(b)]. The temperature dependence of $(1/T_1T)_d/K_d$ and $(1/T_1T)_d/K_d^{3/2}$ are shown in Fig. 2(c). The in-plane values of $(1/T_1T)_d/K_d$ and $(1/T_1T)_d/K_d^{3/2}$ are independent of temperature, and it is difficult to determine the dimensionality of the ferromagnetic fluctuations using only these plots. At present, there is no general theory for numerically analyzing the quasi-two-dimensional system. We discuss the anisotropic spin fluctuations including its two dimensionality from the parameters, which are independently estimated using three-dimensional ferromagnetic SCR theory for each field direction. We first estimate the spin-fluctuation parameter using

$$\frac{1}{T_1TK} = \frac{1}{T_1TA\chi} = \frac{3\gamma_n^2 A}{4\pi T_0}, \tag{3}$$

where T_0 is the energy width of the dynamical spin-fluctuation spectrum [20,23]. The parameter T_0 corresponds to the stiffness in amplitude of the spin density [24], and a larger T_0 value mainly implies a larger longitudinal fluctuation of the spin density.

The estimated T_0 values for both in plane and out of plane are 837 and 301 K, respectively. The ratio of T_0^{in} and T_0^{out} is $T_0^{in}/T_0^{out} = 2.78$, indicating anisotropy in spin fluctuations for $SrCo_2P_2$. This result contrasts that for $LaCo_2P_2$, which exhibits isotropic T_0 values of 890 and 928 K [22]. Therefore, spin fluctuations in $SrCo_2P_2$ are inferred to have a two-dimensional rather than a three-dimensional character.

B. Single crystals of $CaCo_2P_2$

The field-swept ^{31}P NMR measurements of $CaCo_2P_2$ using its single crystals were performed with the same condition with $SrCo_2P_2$ as described in Sec. III A. From the spectra at each temperature [Fig. 3(a)], the spectral width broadens in accordance with $\chi(T)$ with decreasing temperature over the range 10 K $\leqslant T \leqslant$ 200 K, but is almost constant below 110 K because of magnetic ordering. The spectra do not show any fine structure in either field direction even below 110 K, which is consistent with the fact that $CaCo_2P_2$ is a A-type antiferromagnet for which the (001) planes of ferromagnetically ordered Co moments stack antiparallel with neighboring (001) planes [15]. From Fig. 3(b), $\chi(T)$ increases with decreasing temperature below the Néel temperature, suggesting that the interlayer antiferromagnetic interaction is much weaker than the dominant intralayer ferromagnetic interaction. The K-χ plot shows good linearity, with A_a and A_c estimated to be 22.67 and 11.89 kOe/μ_B, respectively. A $A_a > A_c$ trend is observed in common with $SrCo_2P_2$.

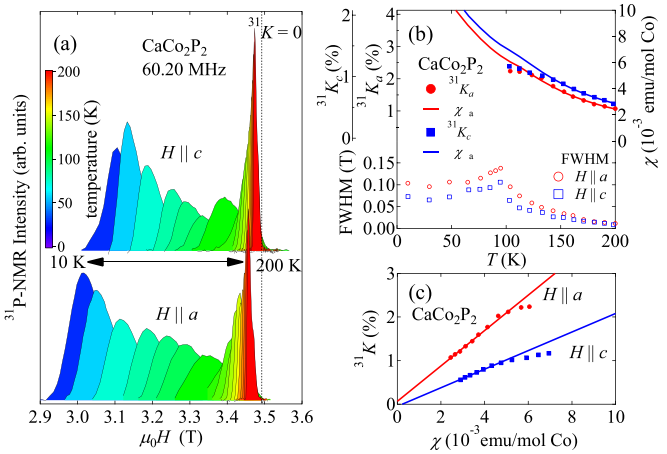

FIG. 3. NMR results for the static susceptibility in single crystals of $CaCo_2P_2$. (a) Field-swept ^{31}P-NMR spectra with the applied field $H \parallel a$ and $H \parallel c$ at 60.20 MHz. (b) Temperature dependence of the Knight shift, magnetic susceptibility (M/H), and the full width at half maximum of the spectra for each field direction. The solid red circles and blue squares represent $^{31}K_a$ and $^{31}K_c$, respectively. The red and blue lines represent H/M_a and H/M_c at 1 T. The open red circles and blue squares denote the full width at half maximum of the spectra for $H \parallel a$ and $H \parallel c$ (c) K-χ plots for each field direction. The red and blue lines represent linear fits in the range from 130–200 K.

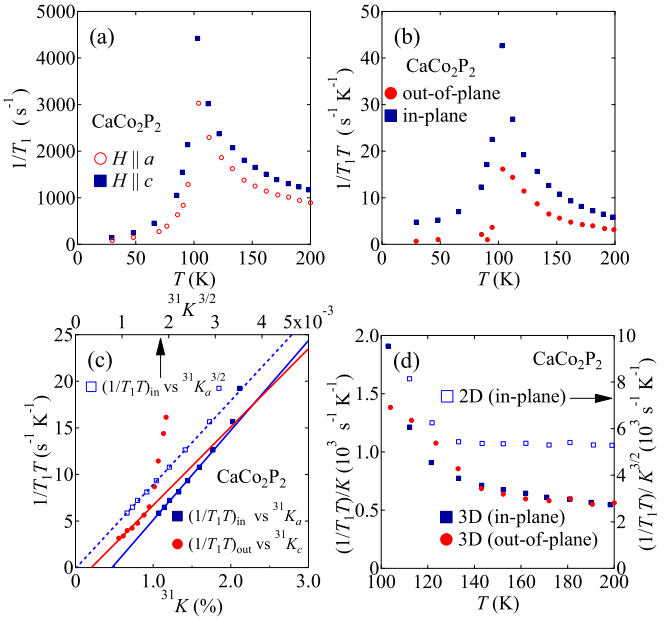

FIG. 4. Dynamical magnetic properties in single crystals of $CaCo_2P_2$. (a) Temperature dependence of $(1/T_1)_a$ and $(1/T_1T)_c$. (b) Temperature dependence of $1/T_1T$. The solid blue squares and the solid red circles distinguish $(1/T_1T)_{in} = (1/T_1T)_c$ and $(1/T_1T)_{out} = 2(1/T_1T)_a - (1/T_1T)_c$, respectively. (c) $1/T_1T$ versus K plots. The solid red circles, the solid blue squares, and the open blue squares represent $(1/T_1T)_{in}$ versus K_a, $(1/T_1T)_{out}$ versus K_c, and $(1/T_1T)_{in}$ versus $K_a^{1.5}$, respectively. The red, blue, and black lines denote linear fits to the data. (d) Temperature versus $1/T_1TK$ and $1/T_1TK^{3/2}$.

Even under a large field of 3 T, the temperature dependence of $1/T_1$ [Fig. 4(a)] exhibits divergent behavior at the magnetic transition temperature $T_N = 110$ K in $CaCo_2P_2$. The value of $1/T_1$ around T_N is double that of the ferromagnetic compound $LaCo_2P_2$ around T_C [22]. This difference results from the fact that $CaCo_2P_2$ has an interlayer antiferromagnetic interaction corresponding to the $\boldsymbol{q} \neq 0$ modes of dynamical susceptibility that are harder to suppress with an external magnetic field than the ferromagnetic $\boldsymbol{q} = 0$ modes.

As mentioned in Sec. III A, the K and $K^{3/2}$ dependence of $1/T_1T$ for $CaCo_2P_2$ [Fig. 4(c)] exhibit good linearity for both in-plane and out-of-plane components suggests that the ferromagnetic mode ($\boldsymbol{q} = 0$) is dominant in the paramagnetic regime, even in $CaCo_2P_2$. From the slopes of the $1/T_1T$-K plots, T_0^{in} and T_0^{out} are estimated to be 150 and 90 K, respectively. As T_0 scales in accordance with the transverse fluctuations, $CaCo_2P_2$ arguably has smaller transverse fluctuations than $SrCo_2P_2$. In addition, the spin fluctuations in $CaCo_2P_2$ are more isotropic than that in $SrCo_2P_2$, corresponding to a three-dimensional cT structure.

C. $Sr_{1-x}Ca_xCo_2P_2$

Figure 5 shows the temperature dependence of the magnetic susceptibility for $Sr_{1-x}Ca_xCo_2P_2$ at $H = 1$ T for various compositions. In the paramagnetic regime ($x \leqslant 0.5$), $\chi(T) = M/H$ has a maximum at T_{max}. As the Ca content x increases, the value of $\chi(T_{max})$ increases and T_{max} decreases. In μ^+SR experiment [25], the sample of $x = 0.5$ is found to show short-range ordering. Thus, its magnetic susceptibility is relatively larger. For itinerant-electron antiferromagnets, a distinct anomaly at T_N appears in the staggered susceptibility, but often not in uniform susceptibility. In the antiferromagnetic regime ($x > 0.5$), $M(T)/H$ shows an anomaly at T_N and increases as T decreases even below T_N, suggesting that the intralayer ferromagnetic interaction is dominant in this system.

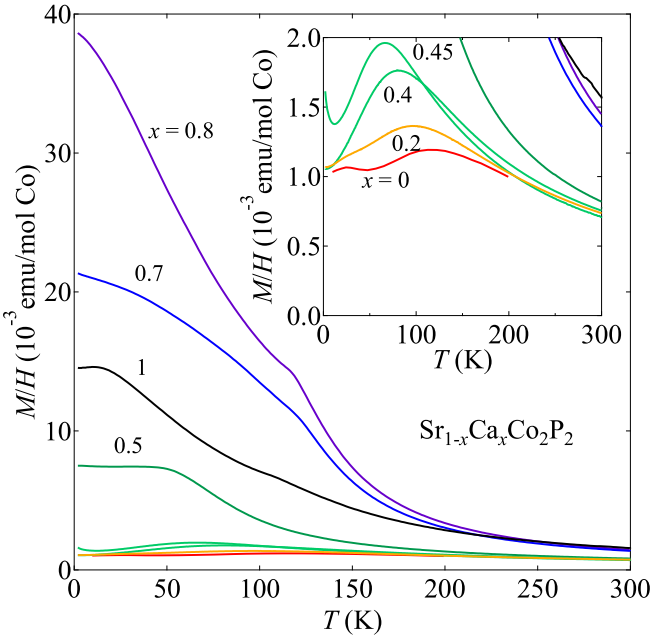

FIG. 5. Temperature dependence of M/H for $Sr_{1-x}Ca_xCo_2P_2$ in a field of 1 T. The inset is a magnification the plot at low susceptibility

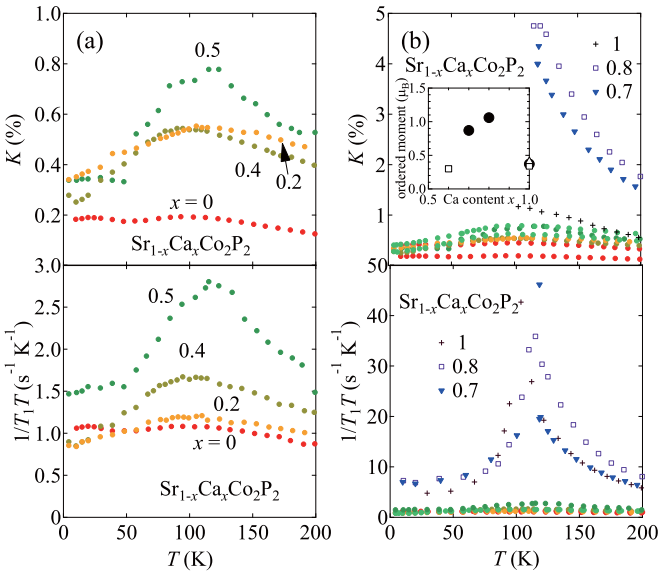

FIG. 6. Temperature dependence of the Knight shift and $1/T_1T$ in $Sr_{1-x}Ca_xCo_2P_2$ for various compositions. (a) Enhanced Pauli paramagnetic regime. (b) Antiferromagnetic regime. The inset in (b) shows the x dependence of the size of ordered Co moment estimated from NMR results (circles), the Arrott plot using magnetization curve (squares), and μSR (triangle) in Ref. [25].

The values of T_N and $M(2K)/H$ have a maximum around $x = 0.8$, which is also found in μ^+SR data [25]. The intralayer ferromagnetic interaction depends on the nearest-neighbor Co-Co distance and/or the Co-P-Co angle of a Co–P tetrahedral layer and becomes larger around $x = 0.85$ [11].

The field-swept ^{31}P NMR measurements of c-aligned samples were performed with operating frequency $\omega = 32.100$ MHz. The temperature dependence of the Knight shift and $1/T_1T$ of the compounds with $0 \leqslant x \leqslant 0.5$ also take maxima at T^*, which are almost independent of x [see Fig. 6(a)]. The values of T^* are different from that of T_{max} in the susceptibility. Since the susceptibility was measured using disoriented powder samples, the difference may reflect a directional dependence in the susceptibility. The maximum absolute values of $1/T_1T$ increase as x increases, suggesting the magnetic interaction also increases as x increases to 0.5.

In contrast, for the compounds with $0.7 \leqslant x \leqslant 1$, the Knight shift and $1/T_1T$ are much larger than those with $0 \leqslant x \leqslant 0.5$, and $1/T_1T$ shows divergent behavior at T_N, suggesting microscopically that these compounds show magnetic ordering. This is consistent with the μ^+SR study in $Sr_{1-x}Ca_xCo_2P_2$ [25]. The size of the ordered moment was estimated from the line width of NMR spectrum at 4.2 K and the hyperfine coupling constant. Here, it is assumed that the hyperfine field mainly comes from the nearest Co atom and the Co moments are aligned in the CoP plane. The size of ordered moment also can be estimated from μSR and magnetization data. Because of the dominant ferromagnetic interaction in this system, the moment size is obtained from the Arrott plot. All the ordered moment sizes are estimated from the above methods [see inset of Fig. 6(b)]. All estimated moment size of $CaCo_2P_2$ are consistent, suggesting the assumption for hyperfine field is appropriate. The x dependence of the moment size has the maximum at $x = 0.8$, and this behavior is associated with the x dependence of Néel temperature and the Co-Co distance, which is proportional to the lattice parameter a [11,13]. In this magnetically ordered region, the moment size and magnetic interaction increases as the Co-Co size increase, which is consistent with a typical ferromagnetic behavior.

The spin fluctuation parameter T_0 of $Sr_{1-x}Ca_xCo_2P_2$ is obtained from the K versus $1/T_1T$ plot using the same method employed in Secs. III A and III B. The hyperfine coupling constant is obtained from the K-χ plot over the high-temperature range. In this case, because the powder sample is c aligned, only the in-plane spin-fluctuation parameter can be obtained.

Figure 7 shows the x dependence of T_0. Recalling that T_0 mainly corresponds to the stiffness of the amplitude of spin density, hence a larger T_0 value means a larger longitudinal fluctuation in the spin density. When T_0 is relatively larger in energy than the magnetic interaction corresponding to the transition temperature, the system has larger longitudinal spin fluctuations, i.e., the system has larger spin fluctuations in its itinerant-electron magnetism.

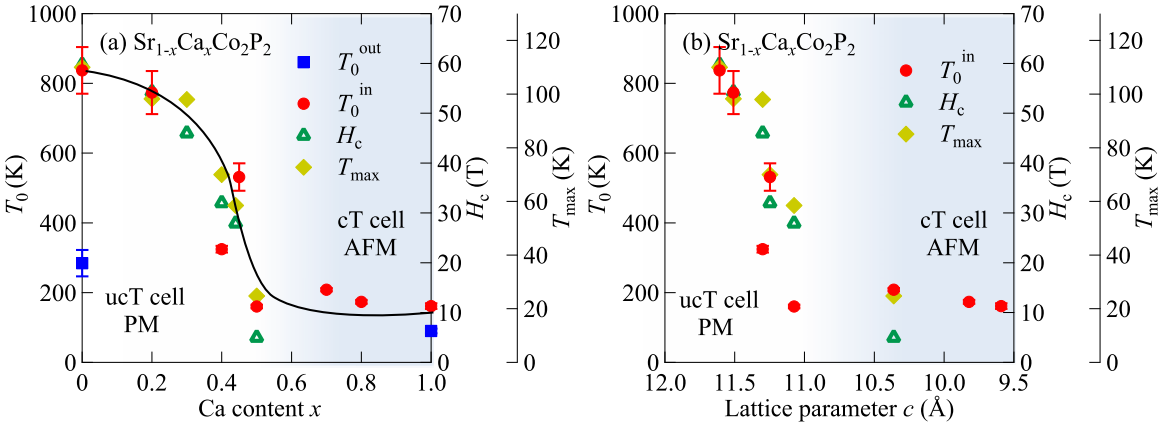

FIG. 7. Spin fluctuation parameter T_0 of $Sr_{1-x}Ca_xCo_2P_2$. (a) T_0 versus Ca content x. (b) T_0 versus lattice parameter c. The circles and squares represent the in-plane and out-of-plane components, respectively, of T_0. The triangles and diamonds represent the metamagnetic transition field H_c and the maximum temperature of the susceptibility T_{max} as in Ref. [13]. The shaded region represents the antiferromagnetic metal (AFM) phase with the collapsed tetragonal (cT) cell.

In the paramagnetic regime with the ucT structure, $SrCo_2P_2$ has large anisotropic T_0, and T_0^{in} is three times larger than T_0^{out}. As x increases to 0.5, the value of T_0^{in} decreases. The structure transforms into the cT structure with interlayer P-P bonds around $x = 0.5$ [11,13]. In the antiferromagnetic regime with the cT structure, the value of T_0 is independent of x and approaches that of T_0^{out} in $CaCo_2P_2$. This x dependence of T_0^{in} implies that T_0^{in} is correlated with the energy associated with characteristic magnetic properties such as the itinerant-electron metamagnetic transition field and T_{max} in $\chi(T)$.

The relationship between the metamagnetic transition and the spin fluctuations has been discussed in other systems. For example, the metamagnetic transition has been related to anisotropic spin fluctuations for the $4f$-electron ferromagnetic system $Ce(Ru_{1-x}Fe_x)PO$ [26]. This metamagnetic CeFePO has two-dimensional interactions and highly anisotropic spin fluctuations; the interaction becomes three dimensional as x decreases to 0.87 at the ferromagnetic quantum critical point [26].

In the present case, spin fluctuations in the metamagnetic compound $SrCo_2P_2$ are anisotropic and they may play an important role in the metamagnetic transition. In particular, interlayer spin fluctuations are directly related to the energy associated with metamagnetic transition, and the value of T_0^{in} scales with the metamagnetic transition field H_c and T_{max} in $\chi(T)$ [see Fig. 7]. According to Takahashi's theory [27], the ratio of the effective magnetic moment and the spontaneous moment p_{eff}/p_s scales with the normalized Curie temperature T_C/T_0 in the three-dimensional itinerant ferromagnetic system, suggesting T_0 depends on the electron itinerancy and the magnetic interaction. For a quasi-two-dimensional system, T_0 tends to become larger as the system becomes more two dimensional [28]. In $Sr_{1-x}Ca_xCo_2P_2$ ($x \leqslant 0.5$), p_s in the ferromagnetic phase under high-magnetic field and p_{eff} are almost independent of x, suggesting the itinerancy does not vary in this regime. In addition, T_0 decreases as x approaches the critical point, suggesting that T_0 does not scale with the magnetic interaction in this case. It is therefore concluded that T_0 reflects the dimensionality of the system.

Finally, we discuss the results from a structural point of view. In the paramagnetic regime ($x \leqslant 0.5$) with a ucT structure, the lattice parameter a is almost independent of x and the nearest neighbor Co-Co distance and the Co-P-Co angle also almost never vary [11]. In contrast, this distance and angle change in the magnetic ordered regime ($x > 0.5$), and the ordered moment and the transition temperature vary with the structural parameters of the Co-P planes [11]. The implication is that the interlayer distance corresponding to c contributes to the magnetic properties such as T_0^{in}, H_c, and T_{max} in the paramagnetic regime. As the interlayer distance decreases under Ca substitution, the intralayer interaction is enhanced. In the quasi-two-dimensional $SrCo_2P_2$, the spin fluctuations are large and anisotropic. The interlayer spin fluctuations are suppressed by development of the three-dimensional interlayer interaction as x increases. For this reason, the ferromagnetic state is stabilized, and as a result, the metamagnetic transition field decreases. Thus, the variation in T_0 and metamagnetic transition field derive from the structure through anisotropic spin fluctuations.

IV. SUMMARY

We have performed ^{31}P NMR measurements $Sr_{1-x}Ca_xCo_2P_2$ at various compositions, and determined the spin fluctuation parameter T_0 corresponding to the frequency spread of the dynamical spin susceptibility using the SCR theory of spin fluctuations. The large frequency spread is associated with a large fluctuation in amplitude of the spin density. As a result, we found that T_0 of the tetragonal ab plane is proportional to the maximum behavior of $\chi(T)$ and the itinerant-electron metamagnetic transition field. In the paramagnetic regime ($0 \leqslant x \leqslant 0.5$), $SrCo_2P_2$ has large fluctuations in the ab plane due to its quasi-two-dimensional ucT structure, and the fluctuations are suppressed by Ca substitution, leading to a collapse along the c-axis direction. In contrast, T_0 is almost invariant with respect to x in the antiferromagnetic regime ($0.5 < x \leqslant 1$) with a cT structure. The interlayer distance between the Co-P planes regulates the spin fluctuations in the ab plane, which moreover play an important role in the occurrence of the metamagnetic transition in this system.

ACKNOWLEDGMENT

This work was supported by JSPS Grant-in-Aid for Scientific Research Grants No. JP26410089 and No. JP16H04131.

[1] M. Rotter, M. Tegel, and D. Johrendt, Phys. Rev. Lett. **101**, 107006 (2008).
[2] A. S. Sefat, R. Jin, M. A. McGuire, B. C. Sales, D. J. Singh, and D. Mandrus, Phys. Rev. Lett. **101**, 117004 (2008).
[3] S. Kasahara, H. Shi, K. Hashimoto, S. Tonegawa, Y. Mizukami, T. Shibauchi, K. Sugimoto, T. Fukuda, T. Terashima, A. H. Nevidomskyy *et al.*, Nature (London) **486**, 382 (2012).
[4] K. Kitagawa, N. Katayama, K. Ohgushi, M. Yoshida, and M. Takigawa, J. Phys. Soc. Jpn. **77**, 114709 (2008).
[5] M. Rotter, M. Tegel, D. Johrendt, I. Schellenberg, W. Hermes, and R. Pöttgen, Phys. Rev. B **78**, 020503 (2008).
[6] Y. Nakai, T. Iye, S. Kitagawa, K. Ishida, H. Ikeda, S. Kasahara, H. Shishido, T. Shibauchi, Y. Matsuda, and T. Terashima, Phys. Rev. Lett. **105**, 107003 (2010).
[7] A. S. Sefat, D. J. Singh, R. Jin, M. A. McGuire, B. C. Sales, and D. Mandrus, Phys. Rev. B **79**, 024512 (2009).
[8] K. Ahilan, T. Imai, A. S. Sefat, and F. L. Ning, Phys. Rev. B **90**, 014520 (2014).
[9] P. Wiecki, V. Ogloblichev, A. Pandey, D. C. Johnston, and Y. Furukawa, Phys. Rev. B **91**, 220406 (2015).
[10] A. Pandey, D. G. Quirinale, W. Jayasekara, A. Sapkota, M. G. Kim, R. S. Dhaka, Y. Lee, T. W. Heitmann, P. W. Stephens, V. Ogloblichev *et al.*, Phys. Rev. B **88**, 014526 (2013).

[11] S. Jia, A. J. Williams, P. W. Stephens, and R. J. Cava, Phys. Rev. B **80**, 165107 (2009).
[12] E. Mörsen, B. Mosel, W. Müller-Warmuth, M. Reehuis, and W. Jeitschko, J. Phys. Chem. Solids **49**, 785 (1988).
[13] M. Imai, C. Michioka, H. Ohta, A. Matsuo, K. Kindo, H. Ueda, and K. Yoshimura, Phys. Rev. B **90**, 014407 (2014).
[14] M. Reehuis, C. Ritter, R. Ballou, and W. Jeitschko, J. Magn. Magn. Mater. **138**, 85 (1994).
[15] M. Reehuis and W. Jeitschko, J. Phys. Chem. Solids **51**, 961 (1990).
[16] R. Hoffmann and C. Zheng, J. Phys. Chem. **89**, 4175 (1985).
[17] S. Jia, P. Jiramongkolchai, M. Suchomel, B. Toby, J. Checkelsky, N. Ong, and R. Cava, Nature Phys. **7**, 207 (2011).
[18] A. J. Millis, Phys. Rev. B **48**, 7183 (1993).
[19] M. Imai, C. Michioka, H. Ueda, A. Matsuo, K. Kindo, and K. Yoshimura, Phys. Procedia **75**, 142 (2015).
[20] T. Moriya, *Spin Fluctuations in Itinerant Electron Magnetism*, Vol. 56 (Springer-Verlag, Berlin, Heidelberg, 1985).
[21] Y. Takahashi, J. Phys. Soc. Jpn. **55**, 3553 (1986).
[22] M. Imai, C. Michioka, H. Ueda, and K. Yoshimura, Phys. Rev. B **91**, 184414 (2015).
[23] A. Ishigaki and T. Moriya, J. Phys. Soc. Jpn. **65**, 3402 (1996).
[24] T. Moriya and Y. Takahashi, J. Phys. Soc. Jpn. **45**, 397 (1978).
[25] J. Sugiyama, H. Nozaki, I. Umegaki, M. Harada, Y. Higuchi, K. Miwa, E. J. Ansaldo, J. H. Brewer, M. Imai, C. Michioka *et al.*, Phys. Rev. B **91**, 144423 (2015).
[26] S. Kitagawa, K. Ishida, T. Nakamura, M. Matoba, and Y. Kamihara, J. Phys. Soc. Jpn. **82**, 033704 (2013).
[27] Y. Takahashi, *Spin Fluctuation Theory of Itinerant Electron Magnetism* (Springer-Verlag, Berlin, 2013).
[28] Y. Takahashi, J. Phys.: Cond. Matt. **9**, 10359 (1997).